INSTINCT

D1.3

Wireless Stochastic Geometry and Stochastic Geometry based JCAS Metrics

INRIA PARIS

Revisions

Work package	WP1
Task	T1.3
Due date	30.6.2025
Submission date	30 June 2025
Deliverable lead	INRIA Paris
Version	V1.0
Authors	François Baccelli (INRIA Paris) and Nahuel Soprano-Loto (INRIA Paris)
Reviewers	Visa Tapio (UOulu)

Contributing partners

AALTO UNIVERSITY
CENTRALE SUPELEC – UNIVERSITÉ PARIS-SACLAY (CS-UPS)
INRIA & INSAL Lyon
NEC LABORATORIES EUROPE GMBH (NEC)
UNIVERSITY OF OULU (UOULU)
UNIVERSITY OF PIRAEUS RESEARCH CENTER (UPRC)

Document editing history

Version	Date	Description	Contributor(s)
1.0	21-05-2025	First complete version of definition of metrics based on stochastic geometry	Visa Tapio Marco Di Renzo Jean Marie Gorce Francesco Devoti Robin Rajamäki Angeliki Alexiou

Document information

Nature of the deliverable*:		R
Dissemination level:		
PU	Public, fully open. e.g., website	✓
SEN	Confidential to INSTINCT project and Commission Services	

* Deliverable types:

R - Document, report

DMP – Data Management Plan

DEM – Demonstrator, pilot, prototype

Disclaimer

Funded by the European Union. Views and opinions expressed are however those of the author(s) only and do not necessarily reflect those of the European Union or SNS JU. Neither the European Union nor the granting authority can be held responsible for them.

Executive Summary

This document provides a theoretical foundation for the study of wireless networks using tools from stochastic geometry, with a particular focus on joint communication and sensing (JCAS). It begins with a concise survey of the mathematical foundations of the field and reviews significant questions that have been addressed so far using this approach in cellular network scenarios.

The main contribution is the definition of a new set of performance metrics, grounded in stochastic geometry, designed to evaluate both communication and sensing capabilities—especially in joint settings. These metrics are intended to guide the analysis and design of next-generation wireless systems where communication and sensing functions must coexist and interact efficiently. The motivation for this work lies in the increasing importance of integrated solutions that optimize resource sharing in spectrum, infrastructure, and processing.

This document plays a crucial role in the project as it serves as the theoretical basis for Deliverables 4.1, 4.3 and 4.4, where these metrics will be implemented and tested in a simulation environment. Deliverable 4.1 is a key milestone, as it translates theoretical developments into a concrete tool for evaluating JCAS performance under realistic scenarios.

The research is still ongoing, particularly concerning the statistical correlations between communication and sensing functions. Additional metrics are also under investigation for future implementation.

The work presented here reflects contributions from multiple INSTINCT partners: Aalto University, CS-UPS, INRIA, NEC, UOULU and UPRC. It situates itself as a core component in the broader effort to develop rigorous, efficient, and analytically grounded evaluation methods for smart wireless systems.

Keywords

Stochastic geometry; Joint communication and sensing performance metrics; Holistic analytical modeling

Contents

1 Introduction

This deliverable surveys the basics of wireless stochastic geometry (SG). The survey part is the object of Sections 2 to 3. In this framework, the positions of network elements are represented as realizations of stochastic point processes, and performance metrics, e.g. coverage or Shannon rate and sensing capacity, are functionals of these processes. Information theoretic performance metrics can then be evaluated as spatial averages. This provides a comprehensive system level analysis of large wireless networks and a reduction of large data sets to a small number of parameters. This in turn allows for network optimization in function of its parameters.

In a second step, the paper describes the new SG research directions pertaining to JCAS. We start with a survey on how to extend the classical metrics pertaining to the communication functionality to metrics appropriate for the sensing functionality. The main novelty is in the definition of joint metrics for JCAS. This is discussed in Section 4. We also explain how to evaluate these SG-based performance metrics.

The last section (Section 5) of the paper is focused on the discussion of further metrics that are mathematically well defined and that could be useful in the context of INSTINCT.

2 Poisson Stochastic Geometry

Poisson Stochastic Geometry leverages a few basic models [1], [2]:

- Spatial Poisson point process, which are used to represent the locations of transmitters;
- Spatial Shot–noise fields, which are used to represent interference;
- Poisson–Voronoi tessellations, which are used to represent "Connection to closest".

2.1 Spatial Point Processes

A spatial point process on $\mathbb{R}^2$, Φ, is a random, finite or countably-infinite collection of points in the space $\mathbb{R}^2$, without accumulation. By 'without accumulation', we mean that every bounded region contains finitely many points.

One can think of a realization Φ of a Point Process (P.P. from now on)

- either as a set of points: $\Phi = \{t_i\} \subseteq \mathbb{R}^2$

- or as a counting measure: $\Phi = \sum_i \varepsilon_{t_i}$ where ε_t is the Dirac measure at t, so that
$$\sum_i f(t_i) = \int_{\mathbb{R}^2} f(t)\, \Phi(\mathrm{d}t).$$
Here f is an arbitrary test function.

2.2 Poisson Point Processes

Let Λ be a locally finite non-null measure on $\mathbb{R}^2$.

Definition 1. Φ is a Poisson Point Process of intensity measure Λ if
$$\Pr\big\{\Phi(A_1) = n_1, \ldots, \Phi(A_k) = n_k\big\} = \prod_{i=1}^{k} \left(e^{-\Lambda(A_i)} \frac{\Lambda(A_i)^{n_i}}{n_i!} \right)$$
for all k and all disjoint sets $A_1, \ldots, A_k$. In this equation, we are treating the realisation of the point process Φ as a counting measure, so $\Phi(A_i)$ represents the number of points inside the region A_i, which is an integer. The quantity $\Lambda(A_i)$ represent the 'measure' of the set A_i according to Λ. We will abreviate Poisson Point Process as PPP, or as PPP(Λ) when the intensity needs to be specified.

A homogeneous PPP of intensity λ is a PPP of intensity measure $\Lambda(\mathrm{d}x) = \lambda\, \mathrm{d}x$, a multiple of Lebesgue measure.

Laplace Functional The Laplace functional of a P.P. Φ is
$$\mathcal{L}_\Phi(f) = \mathbb{E}\left[\exp\left(-\int_{\mathbb{R}^2} f(x)\, \Phi(\mathrm{d}x) \right) \right], \quad f \text{ non-negative.}$$

Proposition 2. The Laplace functional of PPP(Λ) is
$$\mathcal{L}_\Phi(f) = \exp\left(-\int_{\mathbb{R}^2} (1 - e^{-f(x)}) \Lambda(\mathrm{d}x) \right).$$

This is useful for evaluating the Laplace transform of the interference created by a PPP.

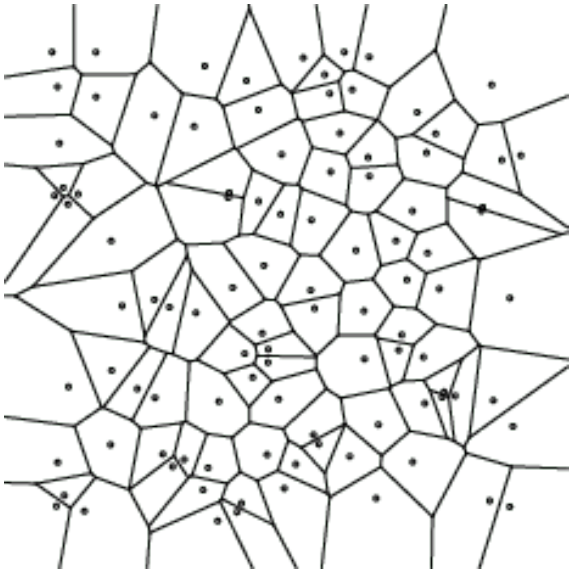

Figure 1: Voronoi tessellation generated by a Poisson point process in $\mathbb{R}^2$.

2.3 Poisson Voronoi Tessellation

For a realisation Φ of the point process, the Voronoi cell $\mathcal{V}^{(t)}(\Phi)$ of atom t of Φ is the set of all locations of $\mathbb{R}^2$ that are closer to t than to any other atom of Φ. Each Voronoi cell is a convex polyhedron of $\mathbb{R}^2$. See Figure 1 for an realisation example.

The empty ball criterion for Voronoi states that $x \in \mathbb{R}^2$ belongs to the Voronoi cell of $t \in \Phi$ iff the open ball of center x and of radius $\|x - t\|$ is empty of points.

If Φ is a PPP with intensity Λ under Palm (i.e. PPP(Λ) plus an atom at 0),

$$\mathbb{P}[x \in \mathcal{V}^{(0)}(\Phi)] = \mathbb{P}[\Phi(\mathcal{B}(x, \|x\|)) = 0] = \exp\{-\Lambda(\mathcal{B}(x, \|x\|))\}.$$

Here $\mathcal{B}(x, \|x\|)$ is the ball of radius $\|x\|$ and center x.

3 Poisson-Voronoi Cellular Networks

Assume that base stations (BSs) are arranged according to a homogeneous Poisson point process of intensity λ in $\mathbb{R}^2$. Users are assumed to be located according to some independent stationary point process. Assume that each

user is served by the closest BS. This leads to service cells which are Poisson Voronoi cells.

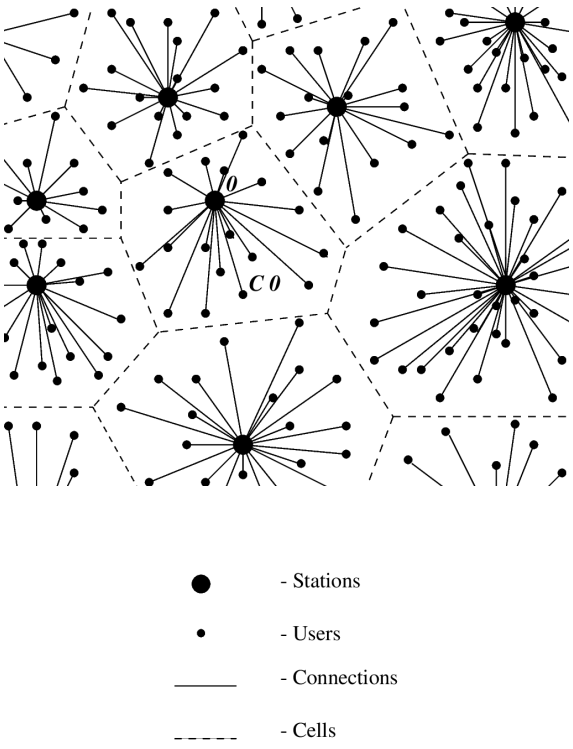

Figure 2: A Poisson-Voronoi-Shannon network.

3.1 Shannon Rate in Poisson-Voronoi Cellular Networks

The Signal-to-Interference-plus-Noise Ratio (SINR) experienced by the typical user is defined by

- The signal power, which stems from the closest BS;
- The interference power, radiated from BSs outside the Voronoi cell of the typical user;
- The thermal noise power N.

The Shannon rate offered to typical user is $\mathcal{T} = B \log(1 + \text{SINR})$, where B stands for the bandwidth. We show below how the law of the Shannon rate offered to typical user can be determined.

Propagation Assumptions Assume the power law path loss model: at distance r, the path loss is

$$l(r) = r^{\beta},$$

with $\beta > 2$ the path loss exponent, which is a classical assumption in real-world environments.

Fading model The fading assumptions are the following:

- Fading on the downlink from BS to tagged user, represented by a random variable S, is Rayleigh with mean $\frac{1}{\mu} = P_{tx}$;
- Fading from other BSs is i.i.d., with representative random variable F with general distribution.

3.2 Coverage and Shannon Rate

Metric 1 within this context is the coverage probability of the typical user:

$$p_c(T, \lambda, \beta) = \mathbb{P}_U^0[\text{SINR} > T] = \mathbb{P}_U^0[\text{Shannon rate} > B \log(1 + T)]. \quad (1)$$

Here, $\mathbb{P}_U^0$ denotes the Palm probability of the user point process [2]. This is equivalent to

- the probability that typical user achieves target T for SINR;
- the average fraction of users who achieve T for SINR;
- the average fraction of the network area in SINR "T-coverage".

Metric 2 is the mean Shannon data rate R of the typical user, defined as

$$\mathbb{E}R = \mathbb{E} \log(1 + \text{SINR}).$$

Note that the bandwidth B is not included in the definition of this metric, as it is considered as a controlled parameter. This metric can be rephrased in equivalent terms as above.

3.3 Poisson–Voronoi–Shannon Formula

Theorem 3 ([4]). The probability of coverage in the cellular network is

$$\begin{aligned} p_c(T, \lambda, \beta) &= \pi\lambda \int_0^{\infty} e^{-\pi\lambda v \kappa(T,\beta) - \mu T N v^{\beta/2}} \mathrm{d}v \\ \kappa(T, \beta) &= \frac{2(\mu T)^{\frac{2}{\beta}}}{\beta} \mathbb{E}\left[F^{\frac{2}{\beta}} \left(\Gamma\left(\frac{-2}{\beta}, \mu T F \right) - \Gamma\left(\frac{-2}{\beta} \right) \right) \right]. \end{aligned}$$

Expectation is with respect to the fading F, and

$$\Gamma(w) = \int_{t=0}^{\infty} \exp(-t)t^{w-1}\mathrm{d}t, \quad \Gamma(w,z) = \int_{t=z}^{\infty} \exp(-t)t^{w-1}\mathrm{d}t.$$

The proof is based on the results listed below only. The signal power is a function of the distance r to the closest BS, which is determined by the empty ball condition. The interference power is characterized by its Laplace transform as the Laplace of the PPP of base stations that are outside the ball of center the UE and of radius r.

3.4 Special Cases

Special Case: $\beta = 4$ Defining

$$Q(x) = \frac{1}{\sqrt{2\pi}} \int_{x}^{\infty} \exp(-y^2/2)\mathrm{d}y,$$

we have

$$\int_0^{\infty} e^{-av}e^{-bv^2}\mathrm{d}v = \sqrt{\frac{\pi}{b}} \exp\left(\frac{a^2}{4b}\right) Q\left(\frac{a}{\sqrt{2b}}\right),$$

and hence

$$p_c(T,\lambda,4) = \frac{\pi^{\frac{3}{2}}\lambda}{\sqrt{T\mu N}} \exp\left(\frac{(\lambda\pi\kappa(T,4))^2}{4T\mu N}\right) Q\left(\frac{\lambda\pi\kappa(T,4)}{\sqrt{2T\mu N}}\right).$$

Special Case: Rayleigh F with the same law as S In this case, we have

$$p_c(T,\lambda,\beta) = \pi\lambda \int_0^{\infty} e^{-\pi\lambda v(1+\rho(T,\beta))-\mu T N v^{\beta/2}}\mathrm{d}v,$$

where

$$\rho(T,\beta) = T^{2/\beta} \int_{T^{-2/\beta}}^{\infty} \frac{1}{1+u^{\beta/2}}\mathrm{d}u.$$

Interference limited sub-case Here we have

$$p_c(T,\lambda,\beta) = \frac{1}{1+\rho(T,\beta)}.$$

Note that, since the right-hand side does not depend on λ, one has a constant coverage probability which is the same for all BS densities!

Special Case: Rayleigh F, $\beta = 4$, interference limited

$$p_c(T, \lambda, 4) = \frac{1}{1 + \sqrt{T}(\pi/2 - \arctan(1/\sqrt{T}))}.$$

3.5 Extensions of the basic Poisson cellular model

3.5.1 Initial Extensions

The following extensions have been considered since [4] (see e.g. [2] and references therein):

- Multi-tier;
- Beyond Rayleigh: Nakagami, Rice;
- Beyond Poisson: Determinantal, Cox;
- Uplink;
- Frequency reuse;
- Resource sharing within cells;
- Power control.

3.5.2 Recent research topics

Here is now a list of more recent research topics:

Cellular densification [5]

- For power law attenuation we have scale invariance;
- For a wide class of bounded attenuation functions Area spectral efficiency $\to 0$ as BS density $\to$ infinity. Hence, there is a sweet spot in terms of BS density.

Shadowing

- Geometry based obstacle shadowing [6] is based on convex stochastic ordering (see Figure 3).
- Obstacle based Shadowing for millimeter wave UE [7], based on multiplicative cascades (see Figure 4).

It is shown in these papers that correlated shadowing is in fact beneficial to wireless spatial averages.

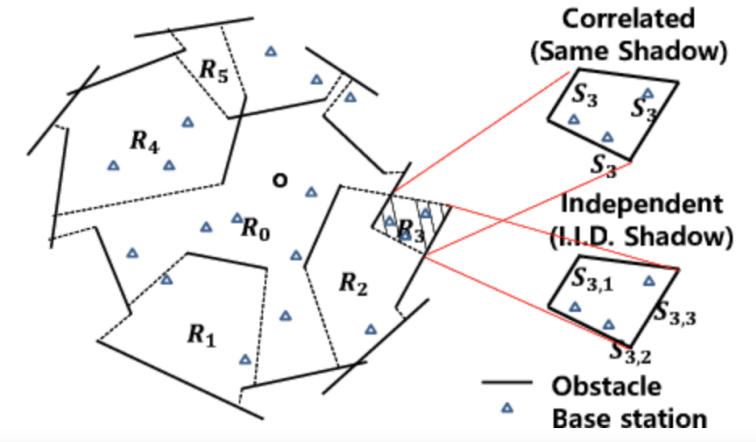

Figure 3: Geometric obstacles.

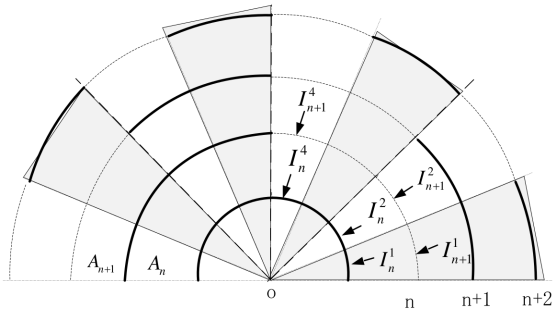

Figure 4: UE centric obstacles.

Beam management The setting of [8] features UEs with several panels and given mobility. The main results are on the optimization of the number/width of beams maximizing the mean effective spectral efficiency, which takes into account both the Shannon rate and the beam handover cost experienced by mobile users.

LEO Constellations NTNs based on LEO satellites require a new cellular geometry with spherical characteristics. It leverages several types of point processes on the sphere:

- Binomial point process or Poisson, like in [9];

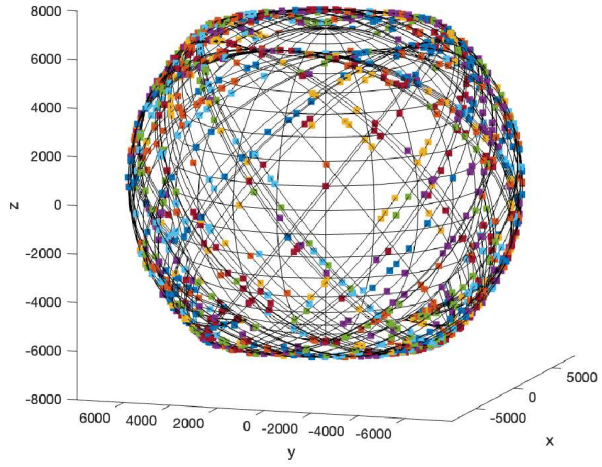

Figure 5: A LEO satellite constellation with 38 degrees inclination orbital planes.

- Cox point processes on Poisson orbits [10].

These papers study downlink coverage and rate of low earth orbit satellite constellations using spherical stochastic geometry.

The objectives of these studies are the analysis of this new type of global radio access and of its cooperation with terrestrial networks.

4 SG Metrics for JCAS

4.1 The SG model

The SG model we propose to use here for an JCAS network is that of [12]. It features Φ_B, Φ_U, Φ_S, which are the Base Station (BS), the User Equipment (UE), and the Sensed Object (SO) point processes, which are independent PPPs with $\lambda_U \gg \lambda_B$ and $\lambda_S \gg \lambda_B$. See Figure 6 for a realisation example. One UE-SO pair is selected at random in the Voronoi cell of each BS.

Each BS transmits data to its UE (the communication part is hence downlink) and at the same time tracks the parameters of interest of its SO using the same frequency bands. The transmit power of the BS is split

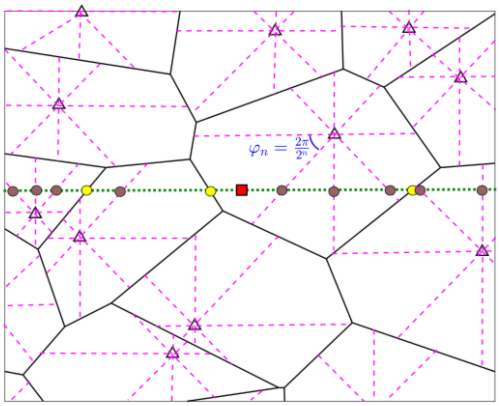

△ : BS locations
■ : UE location
● : Beam reselection locations
● : BS handover locations

Figure 6: Beam Management. Dashed lines: Beam boundaries; Solid lines: Voronoi boundaries

between these two functionalities. The split ratio is one of the parameters of the model.

We have defined (and characterized) in Subsection 3.2 the coverage probability and the Shannon rate of the typical UE. Let us now do the same for the SO, assuming that the variables of interest concerning it evolve according to a linear Gauss-Markov model and that these variables are observed by the BS via a measurement sequence, which is typically a linear transformation of these variables with additive Gaussian noise. Based on these measurements, the BS iteratively maintains a belief (conditional expectation) on the variables of interest and tracks the first moment and the covariance matrix of this belief through an extended Kalman filter. This Kalman filter leverages the parameters of the Gauss Markov model and those of the observation process.

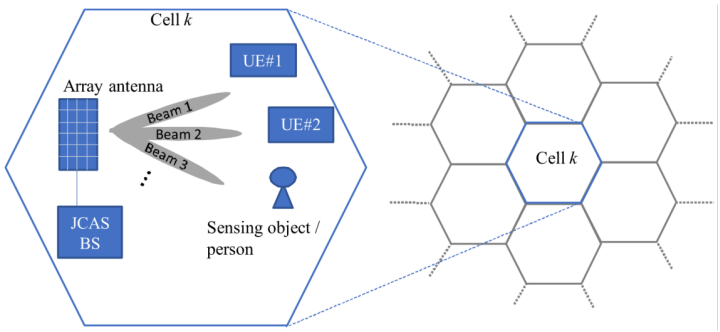

Figure 7: Joint Design of Communication and Sensing for Beyond 5G and 6G Systems," by T. Wild, V. Braun, and H. Viswanathan, published in IEEE Access under the Creative Commons Attribution 4.0 International License (CC BY 4.0).

4.2 Sensing performance metrics

4.2.1 Sensing capacity

Sensing capacity quantifies the rate at which a radar system reduces uncertainty about target parameters (e.g., range, angle) by measuring the mutual information between the true parameters and their noisy estimates. It therefore directly reflects estimation performance, with higher sensing capacity indicating faster reduction in uncertainty. Sensing capacity is defined [13] by

$$C_{\text{rad}} := \frac{I(\boldsymbol{\theta} + \boldsymbol{N}_{\text{est}}; \boldsymbol{\theta})}{T_{\text{CPI}}} \approx \frac{1}{2T_{\text{CPI}}} \log_2(|\mathbb{I} + \boldsymbol{Q}^{1/2}\boldsymbol{R}^{-1}\boldsymbol{Q}^{1/2}|),$$

where $|K|$ denotes the determinant of K.

Here,

- $\boldsymbol{\theta}$ is the vector of unknown target parameters (for instance range and velocity);
- $I(\cdot\,;\cdot)$ denotes mutual information;
- T_{CPI} is the processing interval;
- The prior $P = \mathcal{N}(\bar{\boldsymbol{\theta}}, \boldsymbol{Q})$ is Gaussian;
- $\boldsymbol{N}_{\text{est}} \sim \mathcal{N}(\boldsymbol{0}, \boldsymbol{R})$ is the vector of estimation noise;
- $\mathbb{I}$ is the identity matrix.

The setting is the following:

- Multicarrier waveform used to sense a single target in the presence of interference from the JCAS network;
- The waveform consists of N_c subcarriers, and the maximum burst duration of the radar excitation signal is N_s multicarrier symbols;
- A subset $S_{\text{rad}} \in \{0,1\}^{N_s \times N_c}$ of these resource elements are used for sensing;
- $\text{SINR}_{m,n}$: the SINR on a resource element.

4.2.2 Sensing capacity bound

The sensing capacity is in general difficult to evaluate because $\boldsymbol{R}$ is difficult to evaluate. As in most papers in the field we will rather focus on $C_{\text{rad}}^{\text{UB}}$ which uses the Fisher Information and is defined as

$$C_{\text{rad}}^{\text{UB}} := \frac{1}{2T_{\text{CPI}}} \log_2(|\mathbb{I} + \boldsymbol{Q}^{1/2}\boldsymbol{J}\boldsymbol{Q}^{1/2}|), \tag{2}$$

where $\boldsymbol{J}$ denotes the Fisher Information of the estimation problem related to sensing. It follows from the Cramer Rao theorem that

$$C_{\text{rad}} \leq C_{\text{rad}}^{\text{UB}}. \tag{3}$$

The next theorem is proved in [12].

Theorem 4. The following bounds hold:

$$\frac{1}{2}\log_2(1 + G \cdot \text{SINR}_{\text{rad}}) \leq T_{\text{CPI}} C_{\text{rad}}^{\text{UB}} \leq \log_2\left(1 + \frac{1}{2}G \cdot \text{SINR}_{\text{rad}}\right),$$

where

$$\text{SINR}_{\text{rad}} = \sum_{(m,n)\in S_{\text{rad}}} \eta_{m,n}\text{SINR}_{m,n}$$

and $\{\eta_{m,n}\}, G$ are constants depending on waveform parameters and prior covariance for θ.

As a direct corollary of this theorem, when SINR_{rad} is small,

$$C_{\text{rad}}^{\text{UB}} \sim \frac{G}{2\log(2)T_{\text{CPI}}}\text{SINR}_{\text{rad}}. \tag{4}$$

4.2.3 Sensing metric

By analogy with the definition in (1), we propose to define the basic SG sensing metric as

$$\mathbb{P}_B^0\Big[\frac{G}{2\log(2)T_{\mathrm{CPI}}}\mathrm{SINR}_{\mathrm{rad}} > T\Big], \tag{5}$$

where T is a positive parameter and where $\mathbb{P}_B^0$ denotes the Palm probability of the BS point process [2]. Note that this metric is only valid in the low SINR regime, which is natural in this setting (the signal power stems from reflections and is hence low power).

This is equivalent to

- the probability that typical SO is sensed by its BS with a $C_{\mathrm{rad}}^{\mathrm{UB}}$ capacity larger than or equal to T;
- the average fraction of SOs (or BSs) which achieve a $C_{\mathrm{rad}}^{\mathrm{UB}}$ capacity larger than or equal to T.

The computational aspects are similar to those discussed in the communication part and we will not discuss them further here.

4.3 JACS performance metrics

Consider now a JCAS setting where each BS splits its power to at the same time communicate with its UE and sense its SO.

4.3.1 Marginals

The marginal metrics defined above in terms of coverage and sensing capacity can be used almost directly, for instance through the coverage metrics

$$\mathbb{P}_U^0(\mathrm{SINR}_{\mathrm{com}} \geq T) \text{ and } \mathbb{P}_B^0\Big(\frac{G}{2\log(2)T_{\mathrm{CPI}}}\mathrm{SINR}_{\mathrm{rad}} \geq S\Big)$$

(T and S being the threshold parameters). The only modifications of JCAS (with respect to the sole Communication or sole Sensing cases considered above) are in the evaluation of the SINRs. Signal power has to be changed to take into account the split of total power between the two functionalities. Interference has also to be evaluated differently in view of the fact that each BS simultaneously communicates and senses and that both operations contribute to the interference seen by the process of interest.

4.3.2 Joint metrics

It is quite important to go beyond marginals and to define joint metrics for JCAS. A key observation for this is that, since there is a bijection between the BSs and the UEs in the model, we have

$$\mathbb{P}_U^0(\mathrm{SINR}_{\mathrm{com},0} \geq T) = \mathbb{P}_B^0(\mathrm{SINR}_{\mathrm{com,UE}} \geq T), \tag{6}$$

where by $\mathrm{SINR}_{\mathrm{com},0}$ we mean the interference seen at the origin (which is a UE under $\mathbb{P}_U^0$), whereas by $\mathrm{SINR}_{\mathrm{com,UE}}$ we mean the interference seen at the UE attached to the origin (which is a BS under $\mathbb{P}_B^0$). We highlight that $\mathbb{P}_B^0$ is the Palm probability for BSs (hence assuming the presence of a BS in the origin), and $\mathbb{P}_U^0$ is the Palm probability of UEs (hence assuming a UE at the origin). The last result follows from the mass transport principle [2].

We are now in a position to define the joint metric, which is simply

$$\mathbb{P}_B^0(\mathrm{SINR}_{\mathrm{com,UE}} \geq T, \mathrm{SINR}_{\mathrm{rad}} \geq S), \tag{7}$$

where (S, T) are parameters. The marginals of this joint PDF are those defined above. This is equivalent to

- the probability that the SO of a typical BS is sensed by its BS with a $C_{\mathrm{rad}}^{\mathrm{UB}}$ capacity larger than or equal to $2\log(2)ST_{\mathrm{CPI}}/G$, and that the UE of that BS is T-covered by the said BS;
- the average fraction of BSs which achieve a $C_{\mathrm{rad}}^{\mathrm{UB}}$ capacity larger than or equal to $2\log(2)ST_{\mathrm{CPI}}/G$ w.r.t. their associated SO and T-coverage for their associated UE.

4.3.3 Derived metrics

The Shannon rate to the UE, which is directly related to the SINR for communication, can be the service rate of a queue, with an arrival point process of packets. The steady state of this queue is an instance of derived metric for the communication functionality. Similarly, the Fisher Information for the SO, which is directly related to the SINR for sensing, can be used in a Kalman filter in charge of an iterative estimation of the variables of interest to the BS. The steady state of this queue is an instance of derived metric for the sensing functionality. This holds for both the marginal distributions and the joint distribution.

4.3.4 Joint tuning (contribution made by UPRC)

The expressions of the marginals can be used to pose and solve optimization problems. Here is a simple instance: let $0 < \eta < 1$. Assume that the constraint $\mathbb{P}_B^0(\mathrm{SINR}_{\mathrm{com,UE}} \geq T) > \eta$ is achievable by some power split. Under the constraint $\mathbb{P}_B^0(\mathrm{SINR}_{\mathrm{com,UE}} \geq T) > \eta$, what can be achieved at best for $\mathbb{E}_B^0(\mathrm{SINR}_{\mathrm{rad}})$?

5 Further metrics

Here are known refinements of the coverage and Shannon rate metrics introduced above:

- Fluctuations of the latter, e.g., Meta distribution, based on conditional probability to be T covered given the environment.
- Non homogeneity case, for example, constellation based NTN where the probability of T coverage and the mean Shannon rate are functions of the latitude of the UE.
- Overhead aware case, for example, in the motion and beamforming case, the effective Shannon rate which takes beam handovers and cell handovers into account.

Natural and fundamentally new metrics can be proposed in the context of INSTINCT. A simple example, which is depicted in 2D in Figure 8, is that of RIS based T coverage extension, which is defined as the *proportion of space* that is T covered in the presence of RISs and not in their absence. This again can be defined mathematically as a spatial average and computed using integral geometry.

5.1 Performance metrics in a certain area (contribution made by NEC)

The simplest way of quantifying the performance of a certain KPI is via the threshold function

$$\mathcal{T}(k,T) = \begin{cases} 1 & \text{if } k \geq T \\ 0 & \text{otherwise} \end{cases},$$

where k denotes the value of the KPI to be evaluated, and T is the threshold taken into account. This approach provides a clear separation between

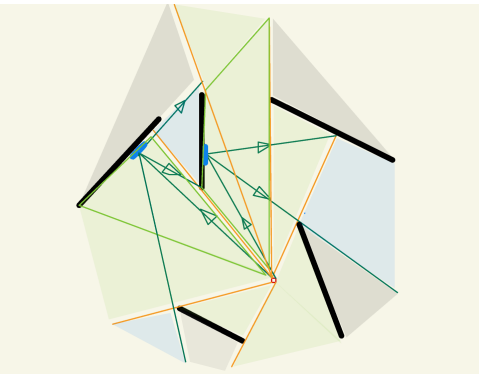

Figure 8: Visibility regions associated with segment-obstacles.

"good" and "bad" performance. For instance, equation (1) can be written as $\mathbb{E}_U^0[\mathcal{T}(\mathrm{SINR}, T)]$.

When the KPI depends on a specific location x of an area of interest A, it is possible to evaluate the goodness of the performance over A —instead of a single point— as

$$\mathcal{D}(A, T) = \frac{1}{|A|} \int_A \mathcal{T}(k(x), T) \mathrm{d}x,$$

denoting $|A|$ the area of A. We quantify in this way the proportion of A delivering at least the desired performance T.

In the context of SG, we can further consider the average of $\mathcal{D}(A, T)$ for a certain region around a typical BS as follows:

$$\mathbb{E}_B^0[\mathcal{D}(A, T)].$$

For example, if A denotes the region that is within a certain distance of the BS, this quantity corresponds to the average fraction of BSs that satisfy the performance criterion defined by T within this surrounding region.

Threshold functions can be also used to evaluate multiple KPIs. For instance, equation (7) can be written as

$$\mathbb{E}_B^0[\mathcal{T}(\mathrm{SINR}_{\mathrm{com,EU}}, T), \mathcal{T}(\mathrm{SINR}_{\mathrm{rad}}, S)]. \tag{8}$$

In the quenched case, i.e. for a fixed realisation of the spatial point process, we can evaluate the joint performance in a certain region A. For instance, if there are n KPIs to be evaluated,

$$\mathcal{D}_{\mathrm{joint}}(A, \bar{T}) = \frac{1}{|A|} \int_A \prod_{i=1}^{n} \mathcal{T}(k(x_i), T_i) \mathrm{d}x_i$$

denotes the proportion of A for which all the KPIs satisfy their dedicated conditions determined by the threshold vector $\bar{T} = (T_1, \ldots, T_n)$. To obtain the average performance of this quantity with respect to a typical UE or BS, it suffices to take expectation with respect to the corresponding Palm distribution.

We finally mention an alternative approach provided by the sigmoid function. For a threshold parameter T, and a control parameter $\beta > 0$, let

$$\mathcal{S}(k, T) = \frac{1}{1 + e^{\beta(T-k)}}. \tag{9}$$

The same analysis we did can be done by substituting $\mathcal{T}$ for $\mathcal{S}$, with the advantage of having a performance metric that is more sensitive in some cases to performance changes.

These area depending metrics are treated in [14] and [15].

6 Conclusions

SG provides a powerful framework for defining a wide range of performance metrics. In this setting, the positions of BSs, UEs and SOs are modeled as realizations of random point processes in space. Performance metrics emerge as functionals of these processes, or as expectations of these functionals under the corresponding probability laws. Thanks to known ergodic properties in SG, it is possible to rigorously characterize the performance of a typical BS or UE, and to study correlations between the performance of different entities, as proposed in Section 4.3.2 in the context of communication-sensing cooperation. Importantly, closed-form expressions can be derived in certain cases, such as those presented in Section 3, illustrating the analytical power of SG in specific network configurations.

References

[1] S.N. Chiu, D. Stoyan, W. Kendall and F. Mecke, "Stochastic Geometry and its Application" Wiley, 2013.

[2] F. Baccelli, B. Blaszczyszyn, M. Karray, "Random Measures, Point Processes, & Stochastic Geometry" `https://hal.inria.fr/hal-02460214`

[3] F. Baccelli and B. Blaszczyszyn, "On a Coverage Process Ranging from the Boolean Model to the Poisson-Voronoi Tessellation", Advances in Applied Probability, 33, pp. 293-323, 2001.

[4] J. Andrews, F. Baccelli, R. Ganti, "A Tractable Approach to Cellular Network Modeling" IEEE Transactions on Communications, Vol. 59, No. 11, pp. 3122-3134, 2011.

[5] A. Alammouri, J. Andrews, F. Baccelli, "Unified Asymptotic Analysis of Area Spectral Efficiency in Ultradense Cellular Networks", IEEE Trans. Information Theory, 65(2): 1236-1248, 2019.

[6] J. Lee, F. Baccelli, "Effect of Shadowing Correlation on Wireless Network Performance", IEEE INFOCOM 2018, Hawai, April 2018.

[7] F. Baccelli, B. Liu, L. Decreusefond, "A User Centric Blockage Model for Wireless Networks", IEEE Trans. Wirel. Commun., 21(10), pp. 8431–8440, 2022.

[8] S. Kalamkar, F. Baccelli, F. Abinader, A. Marcano, L. Uzeda, "Beam Management in 5G: A Stochastic Geometry Analysis", IEEE Transactions on Wireless Communications, 21(4), pp 2275-2290, 2022.

[9] N. Okati, T. Riihonen, D. Korpi, I. Angervuori, R. Wichman, "Downlink coverage and rate analysis of low earth orbit satellite constellations using stochastic geometry" IEEE Transactions on Communications 68 (8), 5120-5134 2020.

[10] C.S Choi, F. Baccelli, "An Analytical Framework for Downlink LEO Satellite Communications based on Cox Point Processes", `https://arxiv.org/abs/2212.03549`

[11] G. Sun, F. Baccelli, K. Feng, S. Paris, L. Uzeda Garcia, "Performance Analysis of RIS-assisted MIMO-OFDM Cellular Networks Based on Matern Cluster Processes", `https://arxiv.org/abs/2310.06754`

[12] N. R. Olson, J. G. Andrews, R. W. Health, Jr, "Coverage and Capacity of Joint Communication and Sensing in Wireless Networks", `https://arxiv.org/abs/2210.02289`, IEEE Tr. Inf. Theory, 2023.

[13] B. Paul, D. W. Bliss, "Extending Joint Radar-Communications Bounds for FMCW Radar with Doppler Estimation", 2015 IEEE Radar Conference (RadarCon), 0089-0094, 2015.

[14] G. Encinas-Lago, F. Devoti, M. Rossanese, V. Sciancalepore, M. Di Renzo, and X. Costa-Pérez, "COLoRIS: Localization-agnostic Smart Surfaces Enabling Opportunistic ISAC in 6G Networks," *IEEE Transactions on Mobile Computing*, 2025.

[15] Y. Lv, S. Liu, Y. Gao, J. Dai, Z. Ren, and Y. Liu, "An ultra-wideband indoor localization algorithm with improved cubature Kalman filtering based on sigmoid function," *Applied Sciences*, vol. 14, no. 6, p. 2239, 2024.

[16] T. Wild, V. Braun and H. Viswanathan, "Joint Design of Communication and Sensing for Beyond 5G and 6G Systems," IEEE Access, vol. 9, pp. 30845–30857, 2021, under CC BY 4.0.